3D human foreskin model for testing topical formulations of sildenafil citrate

Greta Camilla Magnano [a,b,*], Marika Quadri [c], Elisabetta Palazzo [c], Roberta Lotti [c], Francesca Loschi [d], Stefano Dall'Acqua [d], Michela Abrami [e], Francesca Larese Filon [a], Alessandra Marconi [c,*], Dritan Hasa [b,*]

[a] Clinical Unit of Occupational Medicine, University of Trieste, Italy
[b] Department of Chemical and Pharmaceutical Sciences, University of Trieste, Italy
[c] DermoLAB, Department of Surgical, Medical, Dental and Morphological Science, University of Modena and Reggio Emilia, Modena, Italy
[d] Department of Pharmaceutical Science and Pharmacology, University of Padova, Italy
[e] Department of Engineering and Architecture, University of Trieste, Italy

ARTICLE INFO

ABSTRACT

Sildenafil citrate is an approved drug used for the treatment of erectile dysfunction and premature ejaculation. Despite a widespread application, sildenafil citrate shows numerous adverse cardiovascular effects in high-risk patients. Local transdermal drug delivery of this drug is therefore being explored as an interesting and noninvasive alternative administration method that avoids adverse effects arised from peak plasma drug concentrations. Although human and animal skin represents the most reliable models to perform penetration studies, they involve a series of ethical issues and restrictions. For these reasons new *in vitro* approaches based on artificially reconstructed human skin or "human skin equivalents" are being developed as possible alternatives for transdermal testing. There is little information, however, on the efficiency of such new *in vitro* methods on cutaneous penetration of active ingredients. The objective of the current study was to investigate the sildenafil citrate loaded in three commercial transdermal vehicles using 3D full-thickness skin equivalent and compare the results with the permeability experiments using porcine skin. Our results demonstrated that, while the formulation plays an imperative role in an appropriate dermal uptake of sildenafil citrate, the D coefficient results obtained by using the 3D skin equivalent are comparable to those obtained by using the porcine skin when a simple drug suspension is applied ($1.17 \times 10^{-10} \pm 0.92 \times 10^{-10}$ cm^2/s vs $3.5 \times 10^2 \pm 3.3 \times 10^2$ cm^2/s), suggesting that in such case, this 3D skin model can be a valid alternative for *ex-vivo* skin absorption experiments.

1. 1 Introduction

Erectile dysfunction (ED) is the inability to maintain and/or attain the erectile state of the penis allowing for sufficient and satisfactory sexual intercourse (Lue et al. 2004). This common clinical disorder has been thought to affect up to 52% of males aged between 40 and 70 years (Feldman et al. 1994). Sildenafil citrate (Viagra®, Pfizer, New York, NY, USA) is an effective and approved molecule used for the treatment of erectile dysfunction (Fink et al. 2002; Salonia et al., 2003; Badwan et al. 2001; Kirby et al., 2013). This drug allows corpus cavernosum smooth muscle to relax, potentiating erections during sexual stimulation, by selectively inhibiting phosphodiesterase type 5 (PDE5) (Ghofrani et al., 2006; Langtry and Markham, 1999; Thompson et al. 2001). Specifically,

the primary mechanism of action of sildenafil involves the inactivation of cyclic guanosine monophosphate (cGMP), the downstream mediator of the vasodilating agent nitric oxide (NO) resulting in smooth muscle relaxation in penile cavernous tissues (Moreland et al., 1998; Andersson and Wagner, 1995; Lau and Ganesan Adaikan, 2006). Sildenafil is rapidly absorbed after oral administration and the time to achieve maximal peak plasma concentration varies from 0.5 to 2 h (De Toni et al. 2018). Due to its poor solubility, however, sildenafil shows a low oral bioavailability (38–41%) that brings to a delayed onset of action, and possible adverse interactions with other drug such as cardiovascular and hypertension effects in high-risk patients (Muirhead et al. 2002; Osman et al. 2006; Zinner 2007). In the last 15–20 years, many studies focused on the safety of sildenafil following oral administration, and raised some

---

issues including cardiovascular deaths in patients, and in some cases suggesting that the treatment with this drug needs to be stopped immediately (Kloner 2000; Tran and Howes 2003; Kontaras et al., 2008; Tracqui et al. 2002). For such reasons, cutaneous application of the citrate salt of sildenafil has been proposed as a noninvasive alternative method (Atipairin et al. 2020; Abdelalim et al., 2020; Elnaggar et al., 2011; Badr-Eldin and Ahmed, 2016; Elnaggar et al., 2011; Akula and Lakshmi, 2018; Farghali and Ahmed, 2015). However, despite the increasing number of studies where several formulations for the transdermal administration of sildenafil have been proposed, studies focusing on the skin permeability of such molecule are missing. In recent years, various *in vitro* models using synthetic skin membranes have been introduced and investigated to rapidly screen the passive transport of a specific molecule through a given membrane (Kansy et al., 1998). The parallel artificial membrane permeation assay (PAMPA) showed a positive correlation between the permeability of various compounds through such membrane and human skin (Ottaviani et al., 2006). Similarly, Magnano et al. (2022b) demonstrated that the permeability of [6]-gingerol following exposure to ginger pure extract using skin mimicking barrier (SMB) was comparable to those obtained by using the porcine skin, suggesting that the new barrier can be a good alternative to *ex-vivo* animal skin for conducting percutaneous penetration experiments. Today, new *in vitro* approaches based on artificially reconstructed human skin or "human skin equivalents (HSE)" are being developed as possible alternative sources of tissue for skin permeation experiments (Neupane et al. 2020; Iliopoulos et al., 2021; Suhail et al. 2019; Westmoreland and Holmes, 2009). HSE is three-dimensional (3D) *in vitro* tissue-engineered human skin, constructed by culturing human keratinocytes and fibroblasts using sophisticated technologies and quality systems (Idrees et al. 2021). These 3D models are physiologically more similar to the native human skin in terms of morphology, lipid composition, differentiation markers (Ponec et al. 2002; Ponec et al. 2000; Netzlaff et al. 2005), and functionality (viability and metabolism) with respect to *ex vivo* human tissues (Bell et al. 1981), representing a highly predictive and reproducible instrument for preclinical evaluations. Moreover, these advanced 3D models allow to study tumors, including malignant melanoma (MM) as reported by Marconi (Marconi et al. 2018), due to their ability to provide an excellent microenvironment that is closer to the *in vivo* situation to investigate the progression and invasion of the tumor, reducing time-consuming associated to animal studies, and to be cost-effective. HSEs are designed to comprise either only the epidermis or both the dermis and epidermis (full-thickness HSEs) (Zhang and Michniak-Kohn, 2012). Currently, *in vitro* commercially available 3D models are epidermal-only models, including EpiSkin[TM], EpiDerm[TM], and SkinEthic[TM]. The use of HSEs have been validated or are under validation as alternative to animal testing methods for the evaluation of chemical and ingredient hazard: skin irritation (OCED TG 439), skin corrosion (OECD TG 431), eye irritation and skin sensitization (EURL ECVAM Status Report on the Development, Validation and Regulatory Acceptance of Alternative Methods and Approaches (2015) and skin absorption experiments (OECD 2004). It is also worth mentioning that the permeability of molecules through 3D skin models is much higher compared to those measured in human skin *ex vivo*, due to less well-developed barriers (Huong et al. 2009). Nevertheless, these skin equivalent models clearly show higher reproducibility of data, reducing the variability between replicates, which is typically present in skin permeation studies using human or animal skin tissues due to the inter-individual and intra-individual (according to site) variations. Interestingly, such 3D skin models seemed to correctly predict the percutaneous absorption rank order of a series of compounds with different physicochemical properties (Van Gele et al. 2011; Doucet et al., 1998; Gay et al. 1992; Michel et al. 1995; Dreher et al. 2002). The validation and implementation of these experimental models as alternative methods in the evaluation of the molecule permeation, therefore, are strongly promoted, representing a promising scientific innovation. The first aim of this work was to study the skin penetration of sildenafil citrate loaded in three commercial transdermal formulations as model vehicles using 3D full-thickness skin equivalent. The second aim was to compare preliminary permeation assays through the new 3D human foreskin model with skin permeation experiments performed using Franz's diffusion cells and porcine ear skin as model membrane, in order to examine 3D full-thickness skin equivalent as useful membrane for transdermal studies. To further support the good comparability between 3D full-thickness skin equivalent and porcine skin we also performed the diffusion experiments of a sildenafil citrate solution (standard aqueous sample). The choice of sildenafil citrate as a model drug to evaluate the 3D model was dictated for several reasons namely (i) our interest on the use of topical formulations as an alternative administration method for penile treatment (ii) at our knowledge the current study represents the first example where the skin penetration of sildenafil citrate is investigated using a 3D human skin equivalent obtained from human foreskin (iii) sildenafil citrate is often preferred to pure sildenafil in commercial formulations for its superior water solubility.

2. Material and methods

2.1. Materials

All chemicals used in this study were of analytical grade. Specifically, acetonitrile (ACN), ethanol, and formic acid were purchased from Sigma-Aldrich (St. Louis, Missouri, USA). Sodium chloride, sodium hydrogenphosphate, and potassium dihydrogenphosphate were obtained from Carlo Erba (Milan, Italy). Water (reagent grade) was produced with a Millipore purification pack system (MilliQ water). The physiological solution used as the receptor fluid was prepared by dissolving 2.38 g of Na_2HPO_4, 0.19 g of KH_2PO_4 and 9 g of NaCl into 1 L of MilliQ water (final pH = 7.35). Dulbecco's Modified Eagle's Medium (DMEM), Ham's F12 and Gold Keratinocyte Basal Medium (KBM) were purchased from Lonza, (Basel, Switzerland); Fetal bovine serum (FBS), Penicillin/Streptomycin/Amphotericin (PSA); L-Glutamine; DMEM/HAM'SF12 composed of insulin (5 µg/mL); transferrin (5 µg/mL), triiodothyronine (2 nM), cholera enterotoxin (0.1 nM), hydrocortisone (0,4 µg/mL), adenine (180 nM) epidermal growth factor (10 ng/mL) from Sigma-Aldrich (Missouri, USA).

2.2. Preparation of three model topical formulations of sildenafil citrate

In order to check the role of formulation on the permeability, sildenafil citrate was incorporated in three preformed commercial transdermal used as model vehicles, and were purchased from Fagron Italia S. r.l. (Bologna, Italy). The composition of the selected model formulations

Table 1
List of the selected formulations and information given by the manufactures in the label related to composition.

FORMULATION	INGREDIENTS
Formulation A	Sildenafil citrate, water, isopropyl myristate, glyceryl monostearate, PEG-40 stearate, stearic acid, isopropyl palmitate, lecithin, simethicone, urea, cetyl alcohol, stearyl alcohol, potassium sorbate E202, benzoic acid, EDTA, butylated hydroxytoluene (BHT), sorbic acid, carbomer, hydrochloric acid E507.
Formulation B	Sildenafil citrate, water, soybean lecithin, caprylic/capric triglyceride, sorbitol, dimethicone, propylen glycol, stearyl alcohol, glyceryl stearate, alcohol, cetearyl alcohol, ceteareth-20, PEG-100 stearate, cetyl esters wax, octyldodecanol, stearth-2, steareth-21, phenoxyethanol, hydroxyethyl acrylate/sodium acryloyldimethyl taurate copolymer, ethylhexylglycerin, magnesium aluminum silicate.
Formulation C	Sildenafil citrate, water, glycerine, C12 −15 alkyl benzoate, glyceryl stearate, PEG-100 stearate, stearic acid, oleic acid, olive oil, phenoxyethanol, dimethicone, hydroxyethyl acrylate/sodium acryloyldimethyl taurate copolymer, caprylic/capric triglyceride, cetyl alcohol, trolamine, tocopheryl acetate, ethylhexylglycerin

is shown in Table 1. Specifically, formulations A and B are liposomal creams with B being more lipophilic, while formulation C is a classic o/w cream. The three formulations were selected since all contain different enhancers such as such isopropyl myristate and isopropyl palmitate (formulation A), short chain alcohols and glycols (formulation B) or olive oil and oleic acid (formulation C) and thus can potentially accelerate the cutaneous permeation of sildenafil citrate (Lane 2013; Williams and Barry, 2004). The dispersion of the active into each formulation was performed through the following procedure: 1.950 mg of sildenafil citrate was added to 25 mL of a specific vehicle (formulation A, B or C) and transferred in 30 mL container. The mixture was stirred using an unguator (Gako unguator, Farmalabor, Italy) for 6 min at 1000 rpm. The resulting product was stored at room temperature. To determine the concentration of sildenafil citrate in each formulation, 0.5 mL of each topic cream (corresponding to a theoretical amount of 38.6 mg of sildenafil citrate) was dissolved in 6.0 mL of 50/50 % (v/v) water/ethanol solution. The sample was stirred for 4 h, filtered through a 0.45 µm polypropylene housing, polytetrafluoroethylene (PTFE) membrane filter (Whatman®) and assayed by HPLC, using a method reported in the paragraph 2.7. The experimental amounts of the active in 0.5 mL of formulations A, B and C were 38.30 ± 0.21 mg, 38.25 ± 0.34 mg and 38.44 ± 0.19 mg, respectively.

2.3. Rheological properties

Rheological properties of the three topical formulations were determined using a stress controlled rotational rheometer (Haake Mars Rheometer, 379–0200 Thermo Electron GmbH, Karlsruhe, Germany) equipped with plate-plate geometry (PP60, diameter = 60 mm) and a Peltier temperature control system. Samples were loaded between devices and all measurements were carried with a fixed gap of 0.5 mm. Viscoelastic properties of the products were analyzed through several rheological tests. Flow experiment was performed at constant temperature T = 25 °C, over a range shear rate of 1 to 1000 s^{-1}. Temperature sweep was carried from 5 to 40 °C at a heating rate of 1 °C/min and an oscillation frequency of 1 Hz. Time sweep was evaluated for 120 s at a fixed frequency and temperature (1 Hz and 37 °C, respectively). Mechanical spectra were obtained using frequency sweep from 0.1 to 100 Hz at 37 °C.

2.4. 3D human skin equivalent

2.4.1. Isolation of primary human fibroblasts

Primary human dermal fibroblasts (hDF) were obtained from foreskins of two different individuals. Samples were collected with written informed consent of patients, according to the Declaration of Helsinki after approval of the Modena Medical Ethical Committee (Prot. 184/10). Isolated cells were cultured in 175-cm^2 flasks as described by Lotti (Lotti et al. 2022) at 37 °C in a 5 % CO$_2$ humidified atmosphere and 95% air incubator. Cell culture medium was Dulbecco's modified Eagle medium (DMEM), supplemented with 5% (v/v) fetal bovine serum (FBS), 2% (v/v) Glutamine, 1% (v/v) Penicillin-Streptomycin-Amphotericin (PSA). The medium was exchanged every 2 days. Fibroblasts were used for up to 8 passages (P8), reaching 70–80% confluency.

2.4.2. Isolation of primary human epidermal keratinocytes

Primary human epidermal keratinocytes (HEK) were isolated from foreskins according to the Modena Medical Ethical Committee (Prot. 184/10) and seeded onto murine 3 T3 fibroblasts, as feeder layers. Cells were cultured in 75-cm^2 flasks in Ham's F12 medium/Dulbecco's modified Eagle medium (DMEM), containing 10% (v/v) fetal bovine serum (FBS), penicillin (100 U/mL), streptomycin (0.1 mg/mL), Glutamine (4 mM), supplemented with a cocktail of adenine (0.18 mM), insulin (5 µg/mL), transferrin (5 µg/mL), hydrocortisone (0.4 µg/mL), triiodothyronine (2 nM), cholera enterotoxin (0.1 nM), epidermal growth factor (10 ng/mL). The medium was exchanged every 2 days.

Keratinocytes were used at low passage (P2) and subcultured at confluency between 70 and 80%.

2.4.3. 3D reconstructed human skin equivalent

The 3D fully-human skin equivalent was generated by successively fabricating a dermal compartment consisting of fibroblasts and a multi-layered, well differentiated epidermal compartment on top of the dermis as summarized in Fig. 1. Polystyrene scaffolds (12-well Alvetex® scaffold inserts, REPROCELL Europe Ltd, Glasgow, UK) were used for the development of 3D skin equivalent, following the protocol described by Zoio (Zoio 2022). In the 12-well insert format, the scaffold has a diameter of 15 mm and an effective area of 1.12 cm^2. The thickness of the 3D skin equivalent was 0.61 mm ± 0.02 mm (mean of three different skin equivalents ± standard deviation).

2.5. Porcine ear skin preparation

Porcine skin was used as a skin model in the penetration test due to its similarity in terms of morphology and permeability to human skin (Schmook et al., 2001; Barbero and Frederick Frasch, 2009; Wester et al. 1998; Simon and Maibach, 2000). Piglet ears were collected immediately after the suppression of the animal and stored at –25 °C on aluminum foil for a period of up to 4 months. On the day of the experiment, the piglet ears were thawed in a physiological solution at room temperature and the skin samples were cut into 4 cm^2 square pieces. The thickness of the skin samples used was measured with a micrometric caliper (Mitutoyo, Roissy en France, France), obtaining an average value of 0.97 ± 0.03 mm. To evaluate skin integrity, Trans Epidermal Water Loss (TEWL) was measured on each skin piece after one hour of equilibration using a Vapometer (Delfin Vapometer, Delfin Technologies, Sweden) already used in our previous work (Magnano et al., 2022a): the average TEWL values of skin samples was found to be below 10 g·m^{-2}·h^{-1} (Guth et al. 2015).

2.6. In -vitro absorption studies

2.6.1. Permeation assay of sildenafil citrate through 3D full skin equivalent

The permeation test for sildenafil citrate from three topical formulations (formulation A, formulation B and formulation C) was investigate and compared with the aqueous suspension of the drug. 3D skin equivalents (200 µm) were transferred into a new six-well plate, where skin penetration study was conducted. The receptor (basolateral)/surrounding compartment was filled with 4.5 mL of physiological solution, touching the tissue from below. The effective skin area for diffusion was 1.12 cm^2. At time 0 (beginning of the experiment), 0.5 mL of each formulation (The experimental amount of the active in 0.5 mL of each formulation is reported in Section 2.2) was carefully applied on the surface of the skin equivalent. This resulted in a theoretical applied dose of sildenafil citrate Q$_0$ = 34.5 mg/cm^2. The plate was subsequently covered, horizontally shaken and maintained at 32 °C, 5% CO$_2$, throughout the experiment (4 h). At pre-specified time intervals (0, 20, 40, 60, 120, 180, and 240 min) 1.0 mL of receptor solution was withdrawn and immediately replaced with an equal volume of fresh buffer. Samples were analyzed by high performance liquid chromatography (HPLC). Experiments were conducted in three replicates.

2.6.2. Permeation and retention study of sildenafil citrate through porcine skin

Skin absorption studies were performed in static diffusion cells according to the OECD guidelines (OECD 2004). The skin pieces were mounted between the donor and receptor chamber of Franz-type static diffusion cells with the *stratum corneum* facing the donor chamber. The effective skin area for diffusion was 0.95 cm^2. The receptor fluid (RF) was composed of a physiological solution that was continuously stirred using a Teflon coated magnetic stirrer. The concentration of the salt in the receptor fluid is approximately the same as that found in the blood.
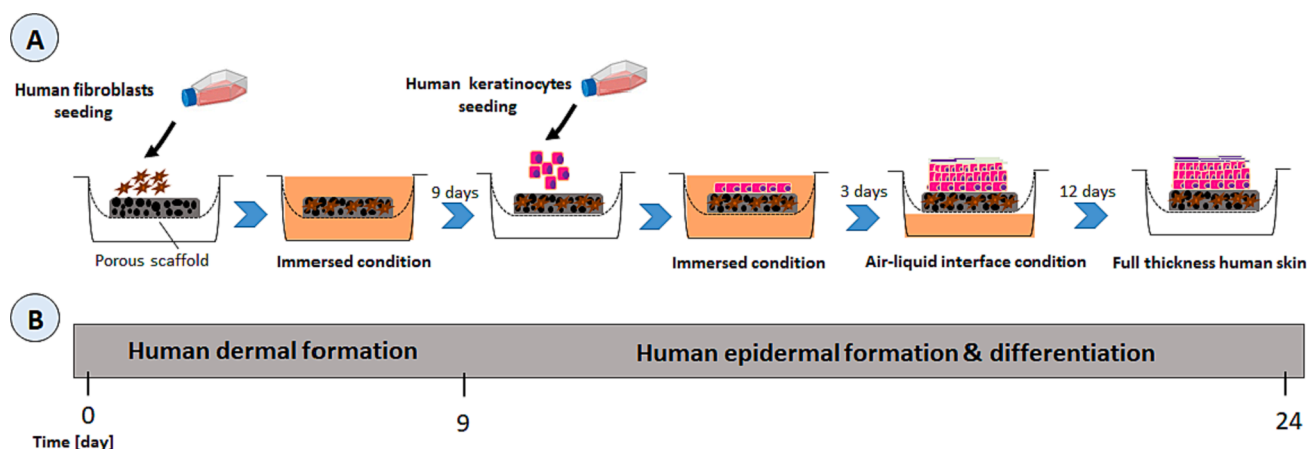
Fig. 1. (A) Schematic representation of the methodology for the development of 3D fully human skin equivalent (HSE). It is generated using a porous polystyrene scaffold seeded with fibroblasts to recreate the dermal layer. Then keratinocytes are seeded on top of the dermal layer and the culture is raised to air liquid interface culture conditions to allow the keratinocytes to differentiate and form epidermal layers. (B): Timeline for the development of HSE.

The receptor compartment had a mean volume of 4.5 mL filled with RF. Mounted Franz cells were maintained at 32 ± 1 °C by means of circulation of thermostated water in the jacket surrounding the cell. At time 0, 0.5 mL of formulation A (corresponding to 38.6 mg of sildenafil citrate) were accurately deposited in direct contact with the porcine skin surface in the Franz cell. This resulted in a theoretical applied dose of sildenafil citrate $Q_0 = 40.6$ mg/cm^2. To assess the absorption experiments, formulation A was selected and was compared with that from drug aqueous suspension. The permeation study lasted 4 h, in order to determine the permeation profile of sildenafil citrate remaining and permeating through the skin. At selected time points (0, 20, 40, 60, 120, 180, and 240 min) 1.0 mL of each receptor sample was collected and analyzed. An equal volume of fresh receptor fluid was immediately replaced in each sample in order to maintain sink conditions. All the experiments were conducted on 3 independent biological replicates. The amounts of sildenafil citrate in RF as well as in each skin layer after 4 h were quantified by HPLC (see later Section 2.7).

2.6.3. Collection and treatment of samples

Ear skin piece was washed three times with 1.0 mL of MilliQ. For each biological sample the *stratum corneum* (SC) was isolated from viable layers by tape stripping (4 strips) using D-Square tape (Monaderm, Monaco) and placed in vials each containing 4.0 mL of MilliQ and stirred for 4 h. Subsequently, the explant epidermis and dermis (E + D) were cut into small pieces with a scalpel, then immersed in 4.0 mL of MilliQ, stirred for 4 h and diluted 1:10 in MilliQ before HPLC analysis. Sildenafil citrate was extracted from each fraction (*stratum corneum*, epidermis + dermis) at room temperature for 4 h. After each extraction, aliquots of 1.0 mL were filtered through a 0.45 μm polypropylene filter (polytetrafluoroethylene (PTFE) membrane filter, Whatman® Maidstone, United Kingdom) before analysis by UV-HPLC. Three replicates were performed for each experiment.

2.7. Analysis of sildenafil citrate by high performance liquid chromatography (HPLC)

For each test, the concentration of sildenafil citrate was obtained using an Agilent 1260 chromatograph (Santa Clara, CA, USA) equipped with a diode array (DAD). Agilent InfinityLab Poroshell 120 C18 (3.0 × 100 mm, 4.0 μm) was used as stationary phase, with temperature set to 23 °C. The mobile phase was composed of acetonitrile (A) and 0.1% formic acid water (B), in gradient elution mode, at a flow rate of 0.4 mL/min, in isocratic phase: 30% A, 70% B. The injection volume was 10 μL, and the detection wavelength was 254 nm. The retention time of sildenafil was at 4.8 ± 0.02 min and the total run time was 8 min. Limit of

quantification (LOQ) and limit of detection (LOD) were 0.12 μg/mL and 0.04 μg/mL respectively.

2.8. Permeability calculations and data analysis

The cumulative amount of permeated drug (dQ, expressed in μg) was plotted as a function of time (dt expressed in s). The linear portion of the slope, corresponding to the steady-state (Hopf et al. 2020) was utilized to calculate the flux according to Eq. (1).

$$J = \frac{dQ}{A*dt} \tag{1}$$

where A represents the surface area of the barrier (expressed in cm^2). The calculated flux was used to calculate the apparent permeability coefficient (P_{app}) as Eq. (2):

$$P_{app} = \frac{J}{C_d} \tag{2}$$

where P_{app} (cm/s) is the apparent permeability coefficient, J (μg/cm^2 per s) is the flux at the steady state and C_d is the drug donor concentration (μg/cm^3). The lag time (t_{lag}) that is the delay time of the first contact of the drug with the skin's surface until a steady state flux is established was calculated as the intercept of the plots. In the simplest case of Fickian diffusion through a homogeneous membrane of thickness (h) t_{lag} is given by Eq. (3) (Hopf et al. 2020)

$$t_{lag} = \frac{h^2}{6D} \tag{3}$$

Furthermore, the diffusion coefficient (D, units of cm^2/s) was calculated utilizing Eq. (4) (Hopf et al. 2020)

$$D = \frac{h^2}{t_{lag}*6} \tag{4}$$

2.9. Histological analysis

The reconstructed tissues were fixed with formalin for 2 h at room temperature, dehydrated, and embedded in paraffin wax to allow for transverse sectioning. Sections were thinly sliced (4 μm thick) using a microtome and these were stained using a hematoxylin and eosin (H&E) stain kit (Vector Laboratories Inc., Burlingame, CA, USA). Staining times were 5 min for hematoxylin and 1 min for eosin. The H&E stained slides were examined with a D-Sight slide scanner (Menarini Diagnostics, Bagno a Ripoli, Firenze, Italy). The thickness of the 3D skin equivalent was measured using ImageJ software (National Institutes of Health,

Bethesda, MD, USA) in 6 microscope fields.

2.10. Statistical analysis

The results are expressed as the quantity permeated per skin surface unit (μg/cm^2). Data from skin absorption experiments were expressed as mean $\pm$ standard deviation (SD). Statistical analysis of differences between two groups were analyzed by Student t-test and those between multiple groups were performed using the analysis of variance (ANOVA, one-way) The significance level was set at $p < 0.05$.

3. Results

3.1. Characterization of the creams: rheological properties

The rheological properties of the three topical bases in which sildenafil citrate was dispersed are reported in Fig. 2. The flow curve and temperature sweep of all the samples present a classical shear thinning behavior with viscosity dropping down by increasing the shear rate. The loading process and the presence of the drug in the formulation did not alter the rheological properties of the bases. However, formulation B presented higher viscosity compared to A and C, possibly due to structural differences between the tested products.

The temperature sweep plot in Fig. 2B showed the formulation dependence on heating. Also in this case, all formulations showed similar behaviour although each formulation presented different values of dynamic moduli. Going into more details, at 5 °C elastic moduli G' were slightly higher than the viscous ones G'', indicating a transition state between solid (G'$\gg$G'') and liquid (G'$\ll$G'') behaviour. The real transition where G'' clearly overcame G' occurred at around 18 °C and systems remained in the sol phase at higher temperatures. The results reported in Fig. 2 are in agreement with data reported in the literature (Atipairin et al. 2020). Finally, similar to the viscosity results reported in Fig. 2A, formulation B showed higher G values compare to the other two formulations.

3.2. Permeation profiles of sildenafil citrate from new topical formulations through 3D skin equivalents

The concentrations of sildenafil citrate loaded into three basic topical formulations and the aqueous suspension in the 3D skin equivalents are reported in Fig. 3. It can be observed that the amount of drug in the basolateral medium increase over time among all the formulations at the end of the contact time (4 h). Notably, the sildenafil citrate from the aqueous suspension showed the highest permeation profile reaching a concentration of 426 $\pm$ 12.3 μg/cm^2 after 4 h suggesting that the molecule can easily cross the 3D full thickness skin when available in

solution. This is an important result confirming that the strategy of the local administration of this molecule is possible. Certainly, a simple aqueous suspension of the sildenafil citrate cannot be suitable for local application, but rather it must be incorporated in appropriate formulations with optimal rheological properties that can release the active with a desired profile. A topical product requires optimization also in terms of texture and affinity. In this context, among the three topical formulations, the amount of sildenafil citrate was particularly high in formulation A and formulation C after 4 h of contact through 3D full-thickness skin samples (217 $\pm$ 17.8 μg/cm^2 and 165 $\pm$ 13.3 μg/cm^2, respectively), while the maximum concentration of the drug reached in the formulation B was 53.9 $\pm$ 28.3 μg/cm^2. A statistically significant difference between drug aqueous suspension and the three topical formulations was found. Importantly, the different RF data of sildenafil citrate at 4 h, obtained by formulation B and the other two creams are also statistically different. However, steady state transdermal flux of sildenafil citrate was found to be close and in the same order of magnitude only for formulation C and formulation A through 3D skin models, ranging from $1.96 \times 10^{-4} \pm 0.76 \times 10^{-4}$ μg/cm^2*s to $2.05 \times 10^{-4} \pm 0.12 \times 10^{-4}$ μg/cm^2*s, and 1 to 2 times higher than those obtained for formulation B ($0.69 \times 10^{-4} \pm 0.38 \times 10^{-4}$ μg/cm^2*s $p < 0.05$, Table 2). The P_{app} (cm/s) of sildenafil citrate from each formulation through 3D skin model was determined dividing the flux at the steady state by the concentration of sildenafil citrate in the donor solution (C_d) (see experimental section 2.8). The drug suspension exhibited the highest value of P_{app} ranging around $9.05 \times 10^{-9} \pm 0.89 \times 10^{-9}$ cm/s, while formulation A and formulation C showed similar values of P_{app} ($5.30 \times 10^{-9} \pm 0.30 \times 10^{-9}$ cm/sec and $5.08 \times 10^{-9} \pm 2.56 \times 10^{-9}$ cm/s, respectively). On the other hand the lowest value of P_{app} was registered for formulation B ($1.79 \times 10^{-9} \pm 0.99 \times 10^{-9}$ cm/s) (Table 2).

3.3. Permeation of sildenafil citrate through porcine ear skin model

To examine the 3D full skin equivalent as a new skin model for skin penetration of molecules, permeation experiments were assessed using porcine ear skin through Franz cell method. Among the three topical creams, formulation A was selected due to its suitable rheological behavior leading to a better release profile of the active thus a higher permeability, observed through 3D skin model. Diffusion experiments of a sildenafil citrate suspension (standard aqueous sample) was also performed. The concentrations of sildenafil citrate from formulation A and from drug water suspension that passed into the receptor per unit area of skin are reported in Fig. 4. Sildenafil citrate permeated through the two skin models, showing the following trend: 3D full skin equivalent drug suspension > 3D full skin equivalent formulation A > porcine ear skin drug suspension > porcine ear skin formulation A (Fig. 4). Specifically, the mean amount of sildenafil citrate from formulation A observed in RF
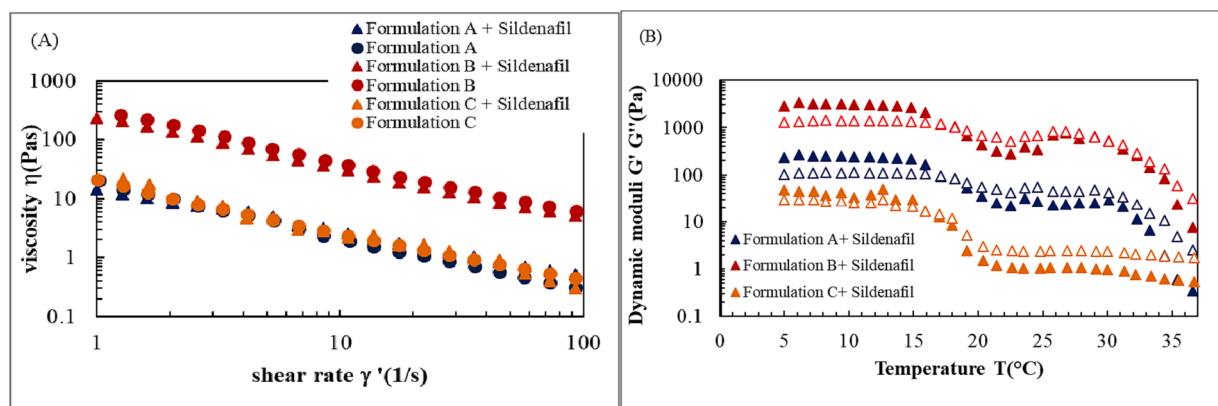

Fig. 2. (A) Flow curve of formulations A(blu), B(red) and C(orange) with and without Sildenafil (triangle and circles respectively); (B) temperature sweep of formulations A(blu), B(red) and C(orange) with drugs, G' was reported with close symbols, G'' with open symbols.
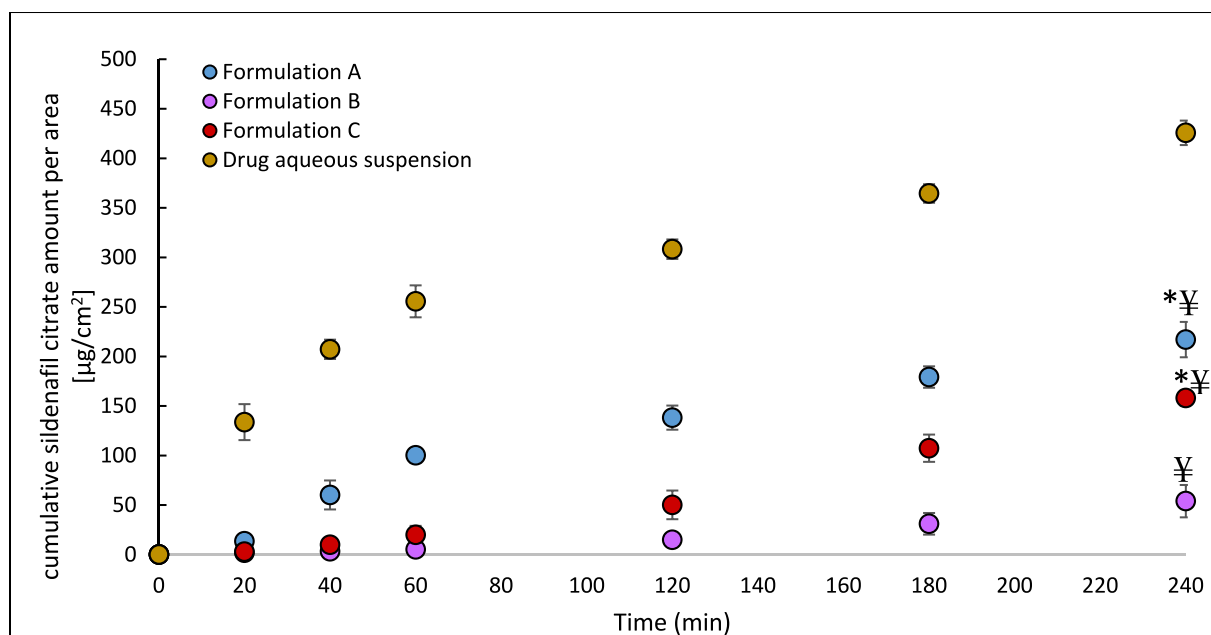
Fig. 3. Sildenafil citrate amount ($\mu g/cm^2$) from topical formulations and from aqueous suspension that permeated in the receptor fluid at specific extraction times through 3D full thickness skin. Values are expressed as mean ± standard error of the mean (SEM) (n = 3). (¥) show the statistically significant differences obtained between aqueous suspension and topical formulations p < 0.05. Asterisk (*) indicates statistically significant differences between formulation B and the other two tested formulations (formulation A and formulation C; p < 0.05).

Table 2
Flux (J), apparent permeability coefficients (P_{app}) and sildenafil citrate concentration loaded into three basic topical formulations and from the aqueous suspension measured for 3D full thickness skin. Values are expressed as mean ± SD (n = 3). (¥) show the statistically significant differences obtained between aqueous suspension and topical formulations p < 0.05. Asterisk (*) indicates statistically significant between formulation B and the other two tested formulations (formulation A and formulation C; p < 0.05).

Formulation	J ($\mu g/cm^2*s$)	P_{app} (cm/s)	Sildenafil citrate concentration in RF at 4 h ($\mu g/cm^2$)
Drug aqueous suspension	2.87×10^{-4} $\pm 0.28 \times 10^{-4}$	9.05×10^{-9} $\pm 0.89 \times 10^{-9}$	426 ± 12.3
Formulation A	2.05×10^{-4} $\pm 0.12 \times 10^{-4}*¥$	5.30×10^{-9} $\pm 0.30 \times 10^{-9}*¥$	$217 \pm 30.9*¥$
Formulation B	0.69×10^{-4} $\pm 0.38 \times 10^{-4}¥$	1.79×10^{-9} $\pm 0.99 \times 10^{-9}¥$	$53.9 \pm 28.3 ¥$
Formulation C	1.96×10^{-4} $\pm 0.76 \times 10^{-4}*¥$	5.08×10^{-9} $\pm 2.56 \times 10^{-9}*¥$	$165 \pm 13.3*¥$

at the end of the contact time (4 h) were 217 ± 30.9 $\mu g/cm^2$ for the 3D full skin equivalent samples and 42.4 ± 24 $\mu g/cm^2$ when porcine ear skin was used. Similarly, the content of sildenafil citrate from aqueous suspension through 3D full skin equivalent samples was higher than those obtained for porcine ear skin (426 ± 12.3 $\mu g/cm^2$ and 358 ± 189 $\mu g/cm^2$, respectively). As it can be seen the different RF data of sildenafil citrate at 4 h, obtained by 3D skin equivalent and the other biological membrane are statistically different. Steady state transdermal fluxes of sildenafil citrate from formulation A and from aqueous suspension through 3D equivalent skin models, however, were found to be 2 times higher than those obtained for porcine ear skin (formulation A: $2.05 \times 10^{-4} \pm 0.12 \times 10^{-4}$ $\mu g/cm^2*s$ *vs* $0.57 \times 10^{-4} \pm 0.33 \times 10^{-4}$ $\mu g/cm^2*s$ p < 0.05; drug suspension $2.87 \times 10^{-4} \pm 0.28 \times 10^{-4}$ $\mu g/cm^2*s$ *vs* $0.99 \times 10^{-4} \pm 0.89 \times 10^{-4}$ $\mu g/cm^2*s$ p < 0.05 Table 3). The P_{app} (cm/s) of sildenafil

citrate through each skin model was determined dividing the flux by the concentration of sildenafil citrate in the donor solution (C_d) (see experimental section 2.8). 3D full skin equivalent produced the highest values of P_{app} ranging around $5.30 \times 10^{-9} \pm 0.30 \times 10^{-9}$ cm/s for formulation A and $9.05 \times 10^{-9} \pm 0.89 \times 10^{-9}$ cm/s for drug suspension compared to those measured through porcine ear skin ($1.48 \times 10^{-9} \pm 0.86 \times 10^{-9}$ cm/s and $3.16 \times 10^{-9} \pm 3.09 \times 10^{-9}$ cm/s, respectively) (Table 3). Importantly, the different diffusion coefficients of the aqueous suspensions of sildenafil citrate obtained by 3D skin equivalent and the porcine skin are $1.17 \times 10^{-10} \pm 0.92 \times 10^{-10}$ cm/s and $3.5 \times 10^2 \pm 3.3 \times 10^2$ cm/s, respectively (p = 0.105). The differences between the two models remain statistically not significant, showing that the two tested models are comparable. On the other hand, the D coefficient of formulation A calculated for porcine ear skin was $5.3 \times 10^2 \pm 0.29 \times 10^2$ cm/s, while $1.06 \times 10^{-10} \pm 0.06 \times 10^{-10}$ cm/s was obtained for 3D skin equivalent (p = 0.005) (Table 3). It is important to underline that a statistically significant difference between the porcine skin and the 3D skin equivalent was found, demonstrating that the two models are not comparable when semisolid products are applied as the case of formulation A.

3.4. Morphological analysis of 3D skin equivalent

The morphology of the developed skin equivalent was analyzed by conducting H&E staining on transverse sections. Fig. 5 shows that the 3D model formed a skin complex architecture with a complete epidermis, mimicking the normal process of epidermal stratification and resembling what has been previously described by Zoio (Zoio 2022). Moreover, the expression of involucrin, critically involved in the formation of the cornified cell envelope, and Claudin-1, a major component of keratinocytes tight junction (TJ) were evaluated to analyze the epidermal barrier formation in the skin equivalent. The results reveal the presence of such typical epidermal tissue protein in the skin equivalent, confirming the epidermal differentiation (Fig. 5).
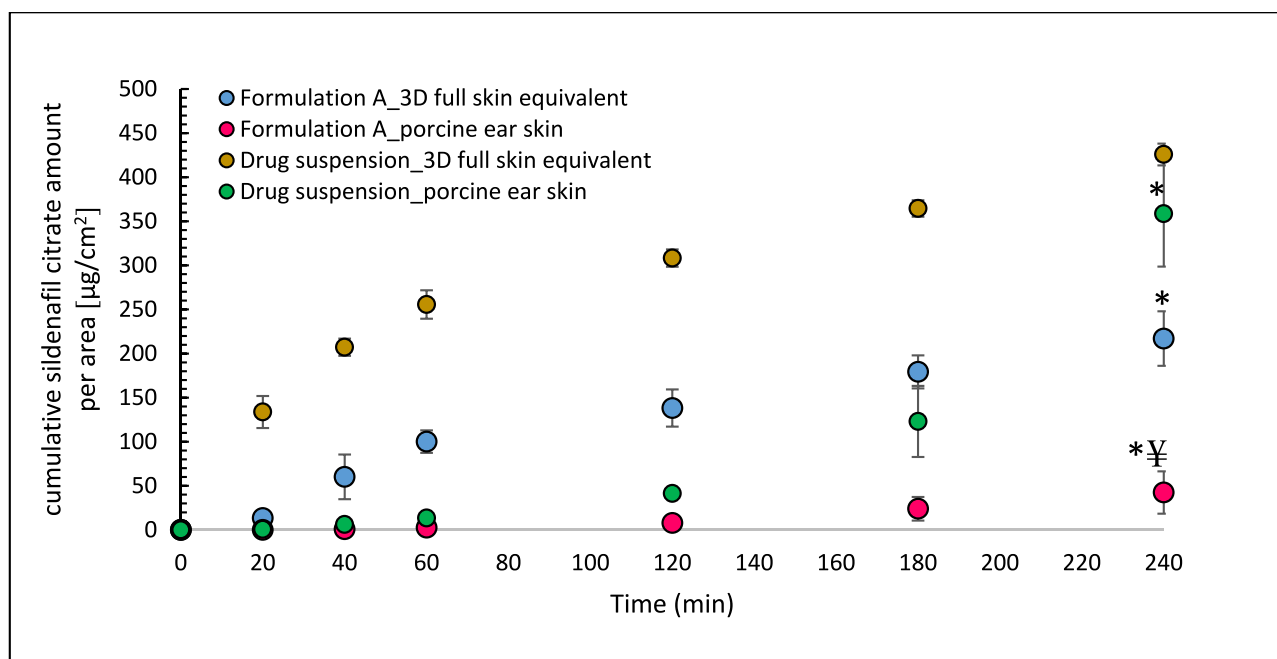
Fig. 4. Sildenafil citrate amount from formulation A and from drug aqueous suspension (μg/cm^2) that permeated in the receptor fluid at specific extraction times through porcine ear skin and 3D full thickness skin. Values are expressed as mean ± SD (n = 3). (¥) show the statistically significant differences obtained between formulation A through 3D skin equivalent and porcine skin p < 0.05. Asterisk (*) indicates statistically significant differences between drug suspension through 3D full thickness skin and the other samples (p < 0.05).

Table 3

Flux (J), apparent permeability coefficients (P$_{app}$), diffusion coefficients (D) and sildenafil citrate concentration loaded in vehicle A and from aqueous suspension measured for each skin model. Values are expressed as mean ± SD (n = 3). (¥) show the statistically significant differences obtained between formulation A through 3D skin equivalent and porcine skin p < 0.05. Asterisk (*) indicates statistically significant between drug suspension through 3D skin equivalent and the other samples (p < 0.05).

Model	J (μg/cm^2*s)	P$_{app}$ (cm/s)	D (cm^2/s)	Sildenafil citrate concentration in RF at 4 h (μg/cm^2)
3D full skin equivalent formulation A	$2.05 \times 10^{-4} \pm 0.12 \times 10^{-4}$ *	$5.30 \times 10^{-9} \pm 0.30 \times 10^{-9}$	$1.06 \times 10^{-10} \pm 0.06 \times 10^{-10}$	217 ± 30.9*
3D full skin equivalent drug suspension	$2.87 \times 10^{-4} \pm 0.28 \times 10^{-4}$	$9.05 \times 10^{-9} \pm 0.89 \times 10^{-9}$	$1.17 \times 10^{-10} \pm 0.92 \times 10^{-10}$	426 ± 12.3
Porcine ear skin formulation A	$0.57 \times 10^{-4} \pm 0.33 \times 10^{-4}$*¥	$1.48 \times 10^{-9} \pm 0.86 \times 10^{-9}$*¥	$5.3 \times 10^2 \pm 0.29 \times 10^2$	42.4 ± 24*¥
Porcine ear skin drug suspension	$0.99 \times 10^{-4} \pm 0.89 \times 10^{-4}$*	$3.16 \times 10^{-9} \pm 3.09 \times 10^{-9}$*	$3.5 \times 10^2 \pm 3.3 \times 10^2$	358 ± 189*

4. Discussion

Pure sildenafil possesses limited water solubility due to its hydrophobic nature and it is classified as Biopharmaceutics Classification System (BCS) class II drug (Kim et al. 2019). As a consequence, the citrate salt form is often preferred in commercial formulation for its superior water solubility (Sawatdee et al. 2019; Doghri et al. 2019; Renshall et al. 2020). Moreover, the salt form is able to guarantee transdermal absorption when administered cutaneously. Indeed, our data demonstrated that the highest amount of sildenafil citrate permeated through 3D skin equivalent was registered for the aqueous drug suspension (Fig. 3 and Table 2). This might be justified by the fact that drug suspension on the skin surface would provide a layer of more concentrated solution in skin pores resulting in higher concentration gradient and increased permeation with time. These results support the choice of the salt form for topical applications and transdermal absorption of sildenafil. The results reported in Fig. 3 and Table 2 showed also the importance of formulation compositions on skin absorption. Among the three topical vehicles, formulation A presented the highest skin permeation of sildenafil citrate. Such observation can be related to the liposomal structure of such formulation that has been already demonstrated to improve transdermal absorption of drugs (Egbaria and Weiner, 1990; Shigeta et al. 2004; Rahimpour and Hamishehkar, 2012). A similar permeation rate was observed when sildenafil citrate was dissolved in the oil-in-water (o/w) emulsion formulation C, which is also an appropriate system for topical application (Otto et al., 2009), allowing the penetration of hydrophilic substances through the *stratum corneum* of the skin (Hoppel et al. 2015). Moreover, it is generally presumed that the penetration of ingredients in an o/w emulsion is higher when they are dissolved in the continuous phase of the emulsion (Wiechers 2005). Since in a typical o/w emulsion the ingredients are mainly distributed into the water continuous phase (Otto et al., 2009) it may be hypothesized that the affinity of sildenafil citrate for some ingredients of formulation C in the continuous phase of the emulsion can apparently facilitate the dermal uptake. An additional reason for the enhanced skin penetration of sildenafil citrate from formulation C can be related to the increase in the hydration level of the *stratum corneum*, caused by exposure to the external aqueous phase of such water-rich emulsion (Otto et al., 2009). Moreover, the positive effect of formulation C may be due to the presence of the olive oil, which act as transdermal enhancer affecting the permeation pathway of the drug (Čižinauskas et al. 2017; Alhasso et al., 2022). Conversely, the skin permeation of sildenafil citrate from formulation B was much lower compared to the other two tested creams (Fig. 3 and Table 2). This may be attributed to the fact that formulation B is a liposomial organogel (lipophilic gel) representing a difficult vehicle for sildenafil citrate to
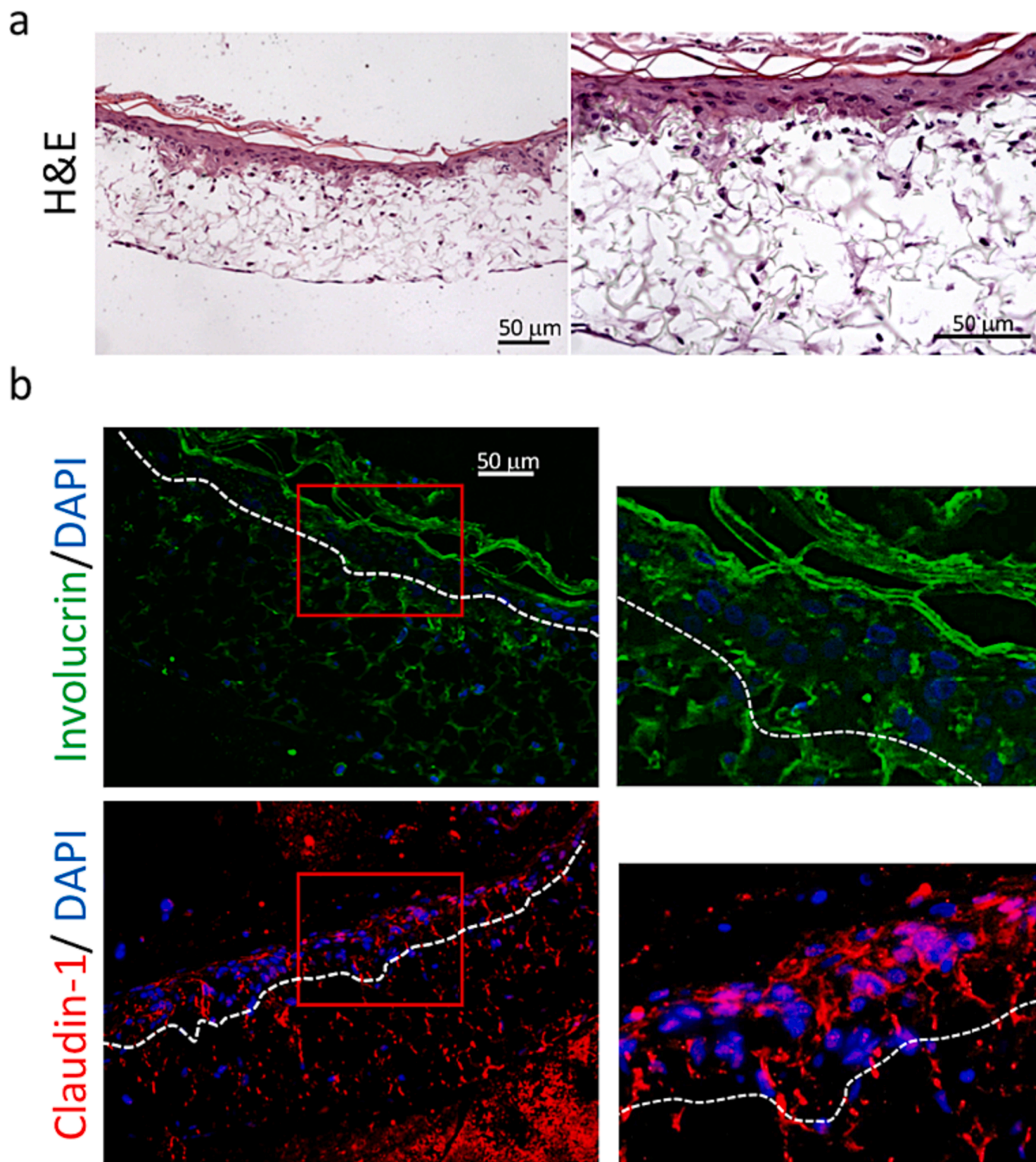
Fig. 5. Histology and evaluation of skin barrier markers expression in 3D skin equivalent. (a): Hematoxilin and Eosin staining. Pictures were taken at 20X (left) and 40X magnification (right). (b): Expression of Involucrin (green) and Claudin-1 (red). Scale bar: 50 μm.

diffuse and eventually cross the skin. Indeed, such formulation presented higher viscosity compare to the other products (Fig. 2). Generally, a highly viscous cream shows low spreadability on the skin, while low viscosity eases the application; in fact, it was reported in the literature a correlation between low viscosity of a vehicle and faster skin penetration of the incorporated drug (Kogan and Garti, 2006). In this work, we explored the potential application of an *in vitro* 3D-human skin

equivalent (3D-HSE) as an alternative method to animal and human testing for assessment of dermal uptake of sildenafil citrate. 3D-HSE was generated by fabricating the dermal and epidermal compartments (Fig. 1) using primary human cells (keratinocytes and fibroblasts) obtained from healthy donors. Cells growing in 3D tissue cultures have different cell surface receptor expression, proliferative capacity, extracellular matrix synthesis, cell density, and metabolic functions that

mimic closely the original human tissue (Brohem et al. 2011). Therefore, skin equivalents should recreate the layers characteristic of the native epidermis: stratum corneum (SC), stratum granulosum (SG), stratum spinosum (SS), and stratum basale (SB) on top of the mature dermis, mimicking the structural and functional properties of native skin as closely as possible (Schäfer-Korting et al. 2008). The *stratum corneum*, is considered as the rate-limiting step for passive drug diffusion across the skin (Scheuplein 1965). Such 3D skin models are preferred in preliminary pharmaceutical studies due to their relative reproducibility, as well as controllable passive transport characteristics (Guenou et al. 2009; Suhail et al. 2019); however, they can also show some limitations including complexity, high cost and the inability to sustain long-term cell culture (Suhail et al. 2019). To compare preliminary permeation assays through this proposed 3D fully-human skin model, the formulation A of sildenafil citrate prepared and the drug suspension were used for assessing the permeation assays through this 3D skin model in comparison to porcine skin in order to examine 3D full-thickness skin equivalent as useful membrane for transdermal studies. The flux values of sildenafil citrate loaded in vehicle A obtained for 3D full thickness skin equivalent was found to be significantly higher compared to those measured for porcine ear skin (Fig. 4 and Table 3). Moreover, the lag time (t_{lag}), the time necessary to establish a linear concentration profile across the barrier was also calculated. Formulation A through porcine ear skin showed a t_{lag} of 93.3 ± 5.1 min, while for 3D skin equivalent the permeation was too rapid and it was not possible to determine t_{lag}. To further support the good comparability between 3D full-thickness skin equivalent and porcine skin we also performed the diffusion experiments of a sildenafil citrate solution (standard aqueous sample). Our results demonstrated higher permeation of drug aqueous suspension through the 3D skin model compared to porcine skin (Fig. 4, Table 3). Similarly, the t_{lag} of drug suspension through the 3D skin equivalent was not possible to determine due to the too fast permeation, while the t_{lag} through porcine ear skin was 62.3 ± 59.3 min. However, the diffusion coefficients of drug suspension measured with the 3D full thickness skin equivalent and the porcine ear skin are not statistically different, showing that the two tested models are comparable (Table 3). On the other hand, when a more complex system is applied such as formulation A, the D values calculated for 3D skin model and porcine skin are statistically different and in such case these two models don't show a positive correlation. The diffusion coefficient (also known as diffusivity) is an essential parameter to understand the passive diffusion through biological barriers and, as a consequence, bioavailability and biodistribution of an active pharmaceutical ingredient (API) (di Cagno et al. 2018). Furthermore, to develop a suitable skin equivalent as valid substitution for drug permeation, the skin barrier function of this model should be similar to *in vivo* healthy human skin. Epidermis barrier formation is associated with involucrin, a cell envelope protein, expressed at an early stage of keratinocyte differentiation (Steven and Steinert, 1994; Candi et al., 2005). This epidermal tissue protein is normally seen only in the upper spinous and granular layers and it promotes envelope formation and cellular cohesion (Candi et al., 2005; Steinert and Marekov, 1997). Additionally, tight junctions (TJs), localized at the SG of the epidermis, are important component of the complex epidermal barrier system and provide mechanical barrier function to ions and solutes of different molecular sizes (Kirschner et al. 2010; Yokouchi et al. 2015). For such reason, the expression of involucrin and claudin-1 at its correct anatomical position was verified in order to demonstrate the correct skin barrier formation and the terminal differentiation of epidermis. The histological evaluation confirms the presence of such typical epidermal tissue protein in our skin model, suggesting the formation of the skin barrier function (Fig. 5). Thus, this good correlation should be attributed to the anatomical characteristics of this 3D skin model generated from foreskins. So based on the evidence, we can conclude that when a simple water drug suspension is applied, such skin models are similar. Finally, it is important to point out that further investigations need to be performed, including an increase of the batches

cells and a wider range of test molecules such as lipophilic compounds as well as other substances with varying physicochemical properties.

5. Conclusion

Our findings demonstrated that the 3D skin equivalent has a positive correlation with ear porcine skin when simple drug suspensions are applied. On the other hand, for more complex and viscous systems such as formulation A, the two tested skin model cannot be considered comparable. Furthermore, it is important to point out the similar anatomical structure of the 3D skin equivalent generated from foreskins with the histological and physiological properties of ear skin barrier. Additionally, the results reported in this study confirmed the importance of the formulation on the dermal permeation of the sildenafil citrate. Although further studies need to be performed, including an expanded panel of substances and pharmaceutical dosage forms, the 3D skin equivalent adopted in this work is able to provide a rapid initial estimation of the amount of sildenafil citrate permeated through the skin, with the potential of being a valid alternative to *ex-vivo* animal skin for skin penetration measurements of new dermal formulations of such important drug.

CRediT authorship contribution statement

Greta Camilla Magnano: Conceptualization, Data curation, Investigation, Writing – original draft. **Marika Quadri:** Data curation, Investigation, Writing – review & editing. **Elisabetta Palazzo:** Investigation, Resources, Writing – review & editing. **Roberta Lotti:** Investigation, Writing – review & editing. **Francesca Loschi:** Investigation. **Stefano Dall'Acqua:** Investigation. **Michela Abrami:** Investigation. **Francesca Larese Filon:** Funding acquisition, Resources. **Alessandra Marconi:** Supervision, Resources, Writing – review & editing. **Dritan Hasa:** Conceptualization, Supervision, Writing – review & editing.

Declaration of Competing Interest

The authors declare that they have no known competing financial interests or personal relationships that could have appeared to influence the work reported in this paper.

Data availability

Data will be made available on request.

References

Abdelalim, L.R., Abdallah, O.Y., Elnaggar, Y.S.R., 2020. High Efficacy, Rapid Onset Nanobiolosomes of Sildenafil as a Topical Therapy for Erectile Dysfunction in Aged Rats. Int. J. Pharm. 591 (décembre), 119978 https://doi.org/10.1016/j.ijpharm.2020.119978.

Akula, P., Lakshmi, P.K., 2018. Effect of pH on weakly acidic and basic model drugs and determination of their ex vivo transdermal permeation routes. Braz. J. Pharm. Sci. 54 (2) https://doi.org/10.1590/s2175-97902018000200070.

Alhasso, B., Ghori, M.U., Conway, B.R., 2022. Systematic Review on the Effectiveness of Essential and Carrier Oils as Skin Penetration Enhancers in Pharmaceutical Formulations. Sci. Pharm. 90 (1), 14. https://doi.org/10.3390/scipharm90010014.

Andersson, K.E., Wagner, G., 1995. Physiology of Penile Erection. Physiol. Rev. 75 (1), 191–236. https://doi.org/10.1152/physrev.1995.75.1.191.

Atipairin, A., Chunhachaichana, C., Nakpheng, T., Changsan, N., Srichana, T., Sawatdee, S., 2020. Development of a Sildenafil Citrate Microemulsion-Loaded Hydrogel as a Potential System for Drug Delivery to the Penis and Its Cellular Metabolic Mechanism. Pharmaceutics 12 (11), 1055. https://doi.org/10.3390/pharmaceutics12111055.

Badr-Eldin, S., Ahmed, O., 2016. Optimized Nano-Transfersomal Films for Enhanced Sildenafil Citrate Transdermal Delivery: Ex Vivo and in Vivo Evaluation. Drug Des. Devel. Ther., avril 1323. https://doi.org/10.2147/DDDT.S103122.

Badwan, A, L Nabuls, M Alomari, N Daraghmeh, et M Ashour. 2001. Sildenafil Citrate. In: Profiles of Drug Substances, Excipients and Related Methodology, 27:339-76. Elsevier. 10.1016/S0099-5428(08)60717-0.

Barbero, A.M., Frederick Frasch, H., 2009. Pig and Guinea Pig Skin as Surrogates for Human in Vitro Penetration Studies: A Quantitative Review. Toxicol. In Vitro 23 (1), 1–13. https://doi.org/10.1016/j.tiv.2008.10.008.

Bell, E., Paul Ehrlich, H., Buttle, D.J., Nakatsuji, T., 1981. Living Tissue Formed in Vitro and Accepted as Skin-Equivalent Tissue of Full Thickness. Science 211 (4486), 1052–1054. https://doi.org/10.1126/science.7008197.

Brohem, C.A., da Silva, L.B., Cardeal, M.T., Soengas, M.S., de Moraes Barros, S.B., et Silvya, S., Maria-Engler, S., 2011. Artificial Skin in Perspective: Concepts and Applications: Artificial Skin. Pigment Cell Melanoma Res. 24 (1), 35–50. https://doi.org/10.1111/j.1755-148X.2010.00786.x.

Cagno, Massimiliano Pio di, Fabrizio Clarelli, Jon Våbenø, Christina Lesley, Sokar Darsim Rahman, Jennifer Cauzzo, Erica Franceschinis, Nicola Realdon, et Paul C. Stein. 2018. Experimental Determination of Drug Diffusion Coefficients in Unstirred Aqueous Environments by Temporally Resolved Concentration Measurements. Mol. Pharmaceut. 15 (4): 1488-94. 10.1021/acs.molpharmaceut.7b01053.

Candi, E., Schmidt, R., Melino, G., 2005. The Cornified Envelope: A Model of Cell Death in the Skin. Nat. Rev. Mol. Cell Biol. 6 (4), 328–340. https://doi.org/10.1038/nrm1619.

Čižinauskas, V., Elie, N., Brunelle, A., Briedis, V., 2017. Skin Penetration Enhancement by Natural Oils for Dihydroquercetin Delivery. Molecules 22 (9), 1536. https://doi.org/10.3390/molecules22091536.

Doghri, Yosra, Fabien Chetaneau, Moez Rhimi, Aicha Kriaa, Valérie Lalanne, Chantal Thorin, Emmanuelle Maguin, M. Yassine Mallem, et Jean-Claude Desfontis. 2019. Sildenafil Citrate Long-Term Treatment Effects on Cardiovascular Reactivity in a SHR Experimental Model of Metabolic Syndrome. Édité par Frank T. Spradley. PLOS ONE 14 (11): e0223914. 10.1371/journal.pone.0223914.

Doucet, O., Garcia, N., Zastrow, L., 1998. Skin Culture Model: A Possible Alternative to the Use of Excised Human Skin for Assessing In Vitro Percutaneous Absorption. Toxicol. In Vitro 12 (4), 423–430. https://doi.org/10.1016/S0887-2333(98)00023-X.

Dreher, F., Fouchard, F., Patouillet, C., Andrian, M., Simonnet, J.-T., Benech-Kieffer, F., 2002. Comparison of Cutaneous Bioavailability of Cosmetic Preparations Containing Caffeine or α-Tocopherol Applied on Human Skin Models or Human Skin Ex Vivo at Finite Doses. Skin Pharmacol. Physiol. 15 (Suppl. 1), 40–58. https://doi.org/10.1159/000066680.

Egbaria, K., Weiner, N., 1990. Liposomes as a Topical Drug Delivery System. Adv. Drug Deliv. Rev. 5 (3), 287–300. https://doi.org/10.1016/0169-409X(90)90021-J.

Elnaggar, Y.S.R., El Massik, M.A., et Ossama, Abdallah, Y., 2011. Sildenafil Citrate Nanoemulsion vs. Self-Nanoemulsifying Delivery Systems: Rational Development and Transdermal Permeation. Int. J. Nanotechnol. 8 (8/9), 749. https://doi.org/10.1504/IJNT.2011.041443.

Elnaggar, Yosra, El-Massik, et Abdallah. 2011. Fabrication, Appraisal, and Transdermal Permeation of Sildenafil Citrate-Loaded Nanostructured Lipid Carriers versus Solid Lipid Nanoparticles. Int. J. Nanomed., décembre, 3195. 10.2147/IJN.S25825.

EURL ECVAM Status Report on the Development, Validation and Regulatory Acceptance of Alternative Methods and Approaches (2015). 2015. Luxembourg: Publications Office of the European Union, 2015. doi:10.2788/62058.

Farghali, R.A., Ahmed, R.A., 2015. Gold Nanoparticles-Modified Screen-Printed Carbon Electrode for Voltammetric Determination of Sildenafil Citrate (Viagra) in Pure Form, Biological and Pharmaceutical Formulations. Int. J. Electrochem. Sci. 10 (2), 1494–1505. https://doi.org/10.1016/S1452-3981(23)05088-5.

Feldman, H.A., Goldstein, I., Hatzichristou, D.G., Krane, R.J., McKinlay, J.B., 1994. Impotence and Its Medical and Psychosocial Correlates: Results of the Massachusetts Male Aging Study. J. Urol. 151 (1), 54–61. https://doi.org/10.1016/S0022-5347(17)34871-1.

Fink, H.A., Donald, R.M., Rutks, I.R., Nelson, D.B., Wilt, T.J., 2002. Sildenafil for Male Erectile Dysfunction: A Systematic Review and Meta-Analysis. Arch. Intern. Med. 162 (12), 1349. https://doi.org/10.1001/archinte.162.12.1349.

Gay, R., Swiderek, M., Nelson, D., Ernesti, A., 1992. The Living Skin Equivalent as a Model in Vitro for Ranking the Toxic Potential of Dermal Irritants. Toxicol. In Vitro 6 (4), 303–315. https://doi.org/10.1016/0887-2333(92)90020-R.

Gele, V., Mireille, B.G., Brochez, L., Speeckaert, R., Lambert, J.o., 2011. Three-Dimensional Skin Models as Tools for Transdermal Drug Delivery: Challenges and Limitations. Expert Opin. Drug Deliv. 8 (6), 705–720. https://doi.org/10.1517/17425247.2011.568937.

Ghofrani, H.A., Osterloh, I.H., Grimminger, F., 2006. Sildenafil: From Angina to Erectile Dysfunction to Pulmonary Hypertension and Beyond. Nat. Rev. Drug Discov. 5 (8), 689–702. https://doi.org/10.1038/nrd2030.

Guenou, H., Nissan, X., Larcher, F., Feteira, J., Lemaitre, G., Saidani, M., Del Rio, M., et al., 2009. Human Embryonic Stem-Cell Derivatives for Full Reconstruction of the Pluristratified Epidermis: A Preclinical Study. Lancet 374 (9703), 1745–1753. https://doi.org/10.1016/S0140-6736(09)61496-3.

Guth, K., Schäfer-Korting, M., Fabian, E., Landsiedel, R., van Ravenzwaay, B., 2015. Suitability of Skin Integrity Tests for Dermal Absorption Studies in Vitro. Toxicol. In Vitro 29 (1), 113–123. https://doi.org/10.1016/j.tiv.2014.09.007.

Hopf, N.B., Champmartin, C., Schenk, L., Berthet, A., Chedik, L., Du Plessis, J.L., Franken, A., et al., 2020. Reflections on the OECD Guidelines for in Vitro Skin Absorption Studies. Regul. Toxicol. Pharm. 117 (novembre), 104752 https://doi.org/10.1016/j.yrtph.2020.104752.

Hoppel, M., Reznicek, G., Kählig, H., Kotisch, H., Resch, G.P., Valenta, C., 2015. Topical Delivery of Acetyl Hexapeptide-8 from Different Emulsions: Influence of Emulsion Composition and Internal Structure. Eur. J. Pharm. Sci. 68 (février), 27–35. https://doi.org/10.1016/j.ejps.2014.12.006.

Huong, S.P., Bun, H., Fourneron, J.-D., Reynier, J.-P., Andrieu, V., 2009. Use of Various Models for in Vitro Percutaneous Absorption Studies of Ultraviolet Filters. Skin Res. Technol. 15 (3), 253–261. https://doi.org/10.1111/j.1600-0846.2009.00368.x.

Idrees, A., Schmitz, I., Zoso, A., Gruhn, D., Pacharra, S., Shah, S., Ciardelli, G., Viebahn, R., Chiono, V., Salber, J., 2021. Fundamental in vitro 3D human skin equivalent tool development for assessing biological safety and biocompatibility –

towards alternative for animal experiments. 4open 4, 1. https://doi.org/10.1051/fopen/2021001.

Iliopoulos, F., Chapman, A., Lane, M.E., 2021. A Comparison of the in Vitro Permeation of 3-O-ethyl-l-ascorbic Acid in Human Skin and in a Living Skin Equivalent (LabSkin™). Int. J. Cosmet. Sci. 43 (1), 107–112. https://doi.org/10.1111/ics.12675.

Kansy, M., Senner, F., Gubernator, K., 1998. Physicochemical High Throughput Screening: Parallel Artificial Membrane Permeation Assay in the Description of Passive Absorption Processes. J. Med. Chem. 41 (7), 1007–1010. https://doi.org/10.1021/jm970530e.

Kim, T.H., Shin, S., Jeong, S.W., Lee, J.B., Shin, B.S., 2019. Physiologically Relevant In Vitro-In Vivo Correlation (IVIVC) Approach for Sildenafil with Site-Dependent Dissolution. Pharmaceutics 11 (6), 251. https://doi.org/10.3390/pharmaceutics11060251.

Kirby, M., Creanga, D.L., Stecher, V.J., 2013. Erectile Function, Erection Hardness and Tolerability in Men Treated with Sildenafil 100 Mg vs. 50 Mg for Erectile Dysfunction. Int. J. Clin. Pract. 67 (10), 1034–1039. https://doi.org/10.1111/ijcp.12229.

Kirschner, N., Houdek, P., Fromm, M., Moll, I., Brandner, J.M., 2010. Tight Junctions Form a Barrier in Human Epidermis. Eur. J. Cell Biol. 89 (11), 839–842. https://doi.org/10.1016/j.ejcb.2010.07.010.

Kloner, R.A., 2000. Cardiovascular Risk and Sildenafil. Am. J. Cardiol. 86 (2), 57–61. https://doi.org/10.1016/S0002-9149(00)00895-X.

Kogan, A., Garti, N., 2006. Microemulsions as Transdermal Drug Delivery Vehicles. Adv. Colloid Interface Sci. 123–126 (novembre), 369–385. https://doi.org/10.1016/j.cis.2006.05.014.

Kontaras, K., Varnavas, V., Kyriakides, Z.S., 2008. Does Sildenafil Cause Myocardial Infarction or Sudden Cardiac Death? Am. J. Cardiovasc. Drugs 8 (1), 1–7. https://doi.org/10.2165/00129784-200808010-00001.

Lane, M.E., 2013. Skin Penetration Enhancers. Int. J. Pharm. 447 (1–2), 12–21. https://doi.org/10.1016/j.ijpharm.2013.02.040.

Langtry, H.D., Markham, A., 1999. Sildenafil: A Review of Its Use in Erectile Dysfunction. Drugs 57 (6), 967–989. https://doi.org/10.2165/00003495-199957060-00015.

Lau, L.-C., Ganesan Adaikan, P., 2006. Mechanisms of Direct Relaxant Effect of Sildenafil, Tadalafil and Vardenafil on Corpus Cavernosum. Eur. J. Pharmacol. 541 (3), 184–190. https://doi.org/10.1016/j.ejphar.2006.05.005.

Lotti, Roberta, Elisabetta Palazzo, Marika Quadri, Marc Dumas, Sylvianne Schnebert, Diego Biondini, Maria Anastasia Bianchini, Carine Nizard, Carlo Pincelli, et Alessandra Marconi. 2022. Isolation of an "Early" Transit Amplifying Keratinocyte Population in Human Epidermis: A Role for the Low Affinity Neurotrophin Receptor CD271. Stem Cells, août, sxac060. 10.1093/stmcls/sxac060.

Lue, T.F., Giuliano, F., Montorsi, F., Rosen, R.C., Andersson, K.-E., Althof, S., Christ, G., et al., 2004. Summary of the Recommendations on Sexual Dysfunctions in Men. J. Sex. Med. 1 (1), 6–23. https://doi.org/10.1111/j.1743-6109.2004.10104.x.

Magnano, Greta Camilla, Stefania Sut, Stefano Dall'Acqua, Massimiliano Pio Di Cagno, Luke Lee, Ming Lee, Francesca Larese Filon, Beatrice Perissutti, Dritan Hasa, et Dario Voinovich. 2022. Validation and Testing of a New Artificial Biomimetic Barrier for Estimation of Transdermal Drug Absorption. Int. J. Pharmaceut. 628 (novembre): 122266. 10.1016/j.ijpharm.2022.122266.

Magnano, G.C., Marussi, G., Filon, F.L., Crosera, M., Bovenzi, M., Adami, G., 2022a. Transdermal Permeation of Inorganic Cerium Salts in Intact Human Skin. Toxicol. In Vitro 82 (août), 105381. https://doi.org/10.1016/j.tiv.2022.105381.

Marconi, A., Quadri, M., Saltari, A., Pincelli, C., 2018. Progress in Melanoma Modelling in Vitro. Exp. Dermatol. 27 (5), 578–586. https://doi.org/10.1111/exd.13670.

Michel, M., Germain, L., Bélanger, P.M., Auger, F.A., 1995. Functional evaluation of anchored skin equivalent cultured in vitro: percutaneous absorption studies and lipid analysis. Pharm. Res. 12 (3), 455–458. https://doi.org/10.1023/A:1016277223852.

Moreland, R.B., Goldstein, I., Traish, A., 1998. Sildenafil, a Novel Inhibitor of Phosphodiesterase Type 5 in Human Corpus Cavernosum Smooth Muscle Cells. Life Sci. 62 (20), PL309–PL318. https://doi.org/10.1016/S0024-3205(98)00158-1.

Muirhead, G.J., Rance, D.J., Walker, D.K., Wastall, P., 2002. Comparative Human Pharmacokinetics and Metabolism of Single-Dose Oral and Intravenous Sildenafil: Single-Dose Pharmacokinetics of Sildenafil. Br. J. Clin. Pharmacol. 53 (février), 13S–20S. https://doi.org/10.1046/j.06-5251.2001.00028.x.

Netzlaff, F., Lehr, C.-M., Wertz, P.W., Schaefer, U.F., 2005. The Human Epidermis Models EpiSkin®, SkinEthic® and EpiDerm®: An Evaluation of Morphology and Their Suitability for Testing Phototoxicity, Irritancy, Corrosivity, and Substance Transport. Eur. J. Pharm. Biopharm. 60 (2), 167–178. https://doi.org/10.1016/j.ejpb.2005.03.004.

Neupane, R., Boddu, S.H.S., Jwala Renukuntla, R., Babu, J., Tiwari, A.K., 2020. Alternatives to Biological Skin in Permeation Studies: Current Trends and Possibilities. Pharmaceutics 12 (2), 152. https://doi.org/10.3390/pharmaceutics12020152.

OECD, 2004. Guideline for the testing of chemicals: skin absorption: in vitro method (n°428).

Osman, M.A., El Maghraby, G.M., Hedaya, M.A., 2006. Intestinal Absorption and Presystemic Disposition of Sildenafil Citrate in the Rabbit: Evidence for Site-Dependent Absorptive Clearance. Biopharm. Drug Dispos. 27 (2), 93–102. https://doi.org/10.1002/bdd.487.

Ottaviani, G., Martel, S., Carrupt, P.-A., 2006. Parallel Artificial Membrane Permeability Assay: A New Membrane for the Fast Prediction of Passive Human Skin Permeability. J. Med. Chem. 49 (13), 3948–3954. https://doi.org/10.1021/jm060230+.

Otto, A., du Plessis, J., Wiechers, J.W., 2009. Formulation Effects of Topical Emulsions on Transdermal and Dermal Delivery. Int. J. Cosmet. Sci. 31 (1), 1–19. https://doi.org/10.1111/j.1468-2494.2008.00467.x.

Ponec, M., Boelsma, E., Weerheim, A., Mulder, A., Bouwstra, J., Mommaas, M., 2000. Lipid and Ultrastructural Characterization of Reconstructed Skin Models. Int. J. Pharm. 203 (1–2), 211–225. https://doi.org/10.1016/S0378-5173(00)00459-2.

Ponec, M., Boelsma, E., Gibbs, S., Mommaas, M., 2002. Characterization of Reconstructed Skin Models. Skin Pharmacol. Physiol. 15 (Suppl. 1), 4–17. https://doi.org/10.1159/000066682.

Rahimpour, Y., Hamishehkar, H., 2012. Liposomes in Cosmeceutics. Expert Opin. Drug Deliv. 9 (4), 443–455. https://doi.org/10.1517/17425247.2012.666968.

Renshall, L.J., Cottrell, E.C., Cowley, E., Sibley, C.P., Baker, P.N., Thorstensen, E.B., Greenwood, S.L., Wareing, M., Dilworth, M.R., 2020. Antenatal Sildenafil Citrate Treatment Increases Offspring Blood Pressure in the Placental-Specific *Igf2* Knockout Mouse Model of FGR. Am. J. Physiol.-Heart Circulatory Physiol. 318 (2), H252–H263. https://doi.org/10.1152/ajpheart.00568.2019.

Salonia, A., Rigatti, P., Montorsi, F., 2003. Sildenafil in Erectile Dysfunction: A Critical Review. Curr. Med. Res. Opin. 19 (4), 241–262. https://doi.org/10.1185/030079903125001839.

Sawatdee, S., Atipairin, A., Yoon, A.S., Srichana, T., Changsan, N., 2019. Enhanced Dissolution of Sildenafil Citrate as Dry Foam Tablets. Pharm. Dev. Technol. 24 (1), 1–11. https://doi.org/10.1080/10837450.2017.1281952.

Schäfer-Korting, M., Bock, U., Diembeck, W., Düsing, H.-J., Gamer, A., Haltner-Ukomadu, E., Hoffmann, C., et al., 2008. The Use of Reconstructed Human Epidermis for Skin Absorption Testing: Results of the Validation Study. Altern. Lab. Anim. 36 (2), 161–187. https://doi.org/10.1177/026119290803600207.

Scheuplein, R.J., 1965. Mechanism of Percutaneous Adsorption. J, Invest. Dermatol. 45 (5), 334–346. https://doi.org/10.1038/jid.1965.140.

Schmook, F.P., Meingassner, J.G., Billich, A., 2001. Comparison of Human Skin or Epidermis Models with Human and Animal Skin in In-Vitro Percutaneous Absorption. Int. J. Pharm. 215 (1–2), 51–56. https://doi.org/10.1016/S0378-5173(00)00665-7.

Shigeta, Y., Imanaka, H., Ando, H., Ryu, A., Oku, N., Baba, N., Makino, T., 2004. Skin Whitening Effect of Linoleic Acid Is Enhanced by Liposomal Formulations. Biol. Pharm. Bull. 27 (4), 591–594. https://doi.org/10.1248/bpb.27.591.

Simon, G.d.A., Maibach, H.I., 2000. The Pig as an Experimental Animal Model of Percutaneous Permeation in Man: Qualitative and Quantitative Observations – An Overview. Skin Pharmacol. Physiol. 13 (5), 229–234. https://doi.org/10.1159/000029928.

Steinert, P.M., Marekov, L.N., 1997. Direct Evidence That Involucrin Is a Major Early Isopeptide Cross-Linked Component of the Keratinocyte Cornified Cell Envelope. J. Biol. Chem. 272 (3), 2021–2030. https://doi.org/10.1074/jbc.272.3.2021.

Steven, A.C., Steinert, P.M., 1994. Protein Composition of Cornified Cell Envelopes of Epidermal Keratinocytes. J. Cell Sci. 107 (2), 693–700. https://doi.org/10.1242/jcs.107.2.693.

Suhail, S., Sardashti, N., Jaiswal, D., Rudraiah, S., Misra, M., Kumbar, S.G., 2019. Engineered Skin Tissue Equivalents for Product Evaluation and Therapeutic Applications. Biotechnol. J. 14 (7), 1900022. https://doi.org/10.1002/biot.201900022.

Thompson, C.S., Mumtaz, F.H., Khan, M.A., Wallis, R.M., Mikhailidis, D.P., Morgan, R.J., Angelini, G.D., Jeremy, J.Y., 2001. The Effect of Sildenafil on Corpus Cavernosal Smooth Muscle Relaxation and Cyclic GMP Formation in the Diabetic Rabbit. Eur. J. Pharmacol. 425 (1), 57–64. https://doi.org/10.1016/S0014-2999(01)01077-9.

De Toni, Luca, Maurizio De Rocco Ponce, Erica Franceschinis, Stefano Dall'Acqua, Roberto Padrini, Nicola Realdon, Andrea Garolla, et Carlo Foresta. 2018. Sublingual Administration of Sildenafil Oro-dispersible Film: New Profiles of Drug Tolerability and Pharmacokinetics for PDE5 Inhibitors. *Frontiers in Pharmacology* 9 (février): 59. 10.3389/fphar.2018.00059.

Tracqui, A., Miras, A., Tabib, A., Raul, J.S., Ludes, B., Malicier, D., 2002. Fatal Overdosage with Sildenafil Citrate (Viagra1): First Report and Review of the Literature. Hum. Exp. Toxicol. 21 (11), 623–629. https://doi.org/10.1191/0960327102ht302oa.

Tran, Diane, et Laurence Guy Howes. 2003. Cardiovascular Safety of Sildenafil: Drug Safety 26 (7): 453-60. 10.2165/00002018-200326070-00002.

Wester, R.C., Melendres, J., Sedik, L., Maibach, H., Riviere, J.E., 1998. Percutaneous Absorption of Salicylic Acid, Theophylline, 2,4-Dimethylamine, Diethyl Hexyl Phthalic Acid, Andp-Aminobenzoic Acid in the Isolated Perfused Porcine Skin Flap Compared to Manin Vivo. Toxicol. Appl. Pharmacol. 151 (1), 159–165. https://doi.org/10.1006/taap.1998.8434.

Westmoreland, C., Holmes, A.M., 2009. Assuring Consumer Safety without Animals: Applications for Tissue Engineering. Organogenesis 5 (2), 67–72. https://doi.org/10.4161/org.5.2.9128.

Wiechers, J.W., 2005. Optimizing Skin Delivery of Active Ingredients From Emulsions. In: Delivery System Handbook for Personal Care and Cosmetic Products. Elsevier, pp. 409–436. https://doi.org/10.1016/B978-081551504-3.50025-0.

Williams, A.C., Barry, B.W., 2004. Penetration Enhancers. Adv. Drug Deliv. Rev. 56 (5), 603–618. https://doi.org/10.1016/j.addr.2003.10.025.

Yokouchi, M., Kubo, A., Kawasaki, H., Yoshida, K., Ishii, K., Furuse, M., Amagai, M., 2015. Epidermal Tight Junction Barrier Function Is Altered by Skin Inflammation, but Not by Filaggrin-Deficient Stratum Corneum. J. Dermatol. Sci. 77 (1), 28–36. https://doi.org/10.1016/j.jdermsci.2014.11.007.

Zhang, Z., Michniak-Kohn, B.B., 2012. Tissue Engineered Human Skin Equivalents. Pharmaceutics 4 (1), 26–41. https://doi.org/10.3390/pharmaceutics4010026.

Zinner, N., 2007. ORIGINAL RESEARCH—ED PHARMACOTHERAPY: Do Food and Dose Timing Affect the Efficacy of Sildenafil? A Randomized Placebo-Controlled Study. J. Sex. Med. 4 (1), 137–144. https://doi.org/10.1111/j.1743-6109.2006.00400.x.

Zoio, P., 2022. Open-source human skin model with an in vivo-like barrier for drug testing. ALTEX. https://doi.org/10.14573/altex.2111182.